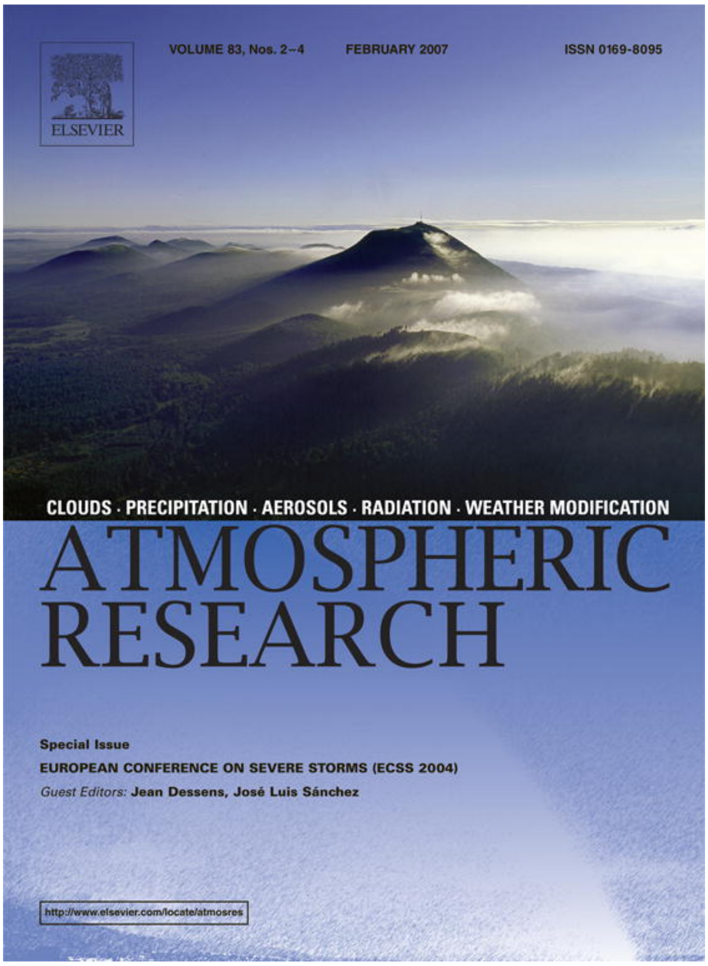
VOLUME 83, Nos. 2–4
FEBRUARY 2007
ISSN 0169-8095
ELSEVIER
CLOUDS · PRECIPITATION · AEROSOLS · RADIATION · WEATHER MODIFICATION
ATMOSPHERIC RESEARCH
Special Issue
EUROPEAN CONFERENCE ON SEVERE STORMS (ECSS 2004)
Guest Editors: Jean Dessens, José Luis Sánchez
http://www.elsevier.com/locate/atmosres

ELSEVIER

Atmospheric Research 83 (2007) 121 – 131

ATMOSPHERIC RESEARCH

www.elsevier.com/locate/atmos

Numerical simulation of severe convective phenomena over Croatian and Hungarian territory

Nataša Strelec Mahović [a,*], Akos Horvath [b,1], Kalman Csirmaz [b,1]

[a] *Meteorological and Hydrological Service, Griè 3, 10 000 Zagreb, Croatia*
[b] *Hungarian Meteorological Service, Storm Warning Observatory, Vitorlas u. 17, H-8600 Siofok, Hungary*

Accepted 29 September 2005

Abstract

Squall lines and supercells cause severe weather and huge damages in the territory of Croatia and Hungary. These long living events can be recognised by radar very well, but the problem of early warning, especially successful numerical forecast of these phenomena, has not yet been solved in this region. Two case studies are presented here in which dynamical modelling approach gives promising results: a squall line preceding a cold front and a single supercell generated because of a prefrontal instability. The numerical simulation is performed using the PSU/NCAR meso-scale model MM5, with horizontal resolution of 3 km. Lateral boundary conditions are taken from the ECMWF model. The moist processes are resolved by Reisner mixed-phase explicit moisture scheme and for the radiation scheme a rapid radiative transfer model is applied. The analysis nudging technique is applied for the first two hours of the model run. The results of the simulation are very promising. The MM5 model reconstructed the appearance of the convective phenomena and showed the development of thunderstorm into the supercell phase. The model results give very detailed insight into wind changes showing the rotation of supercells, clearly distinguish warm core of the cell and give rather good precipitation estimate. The successful simulation of convective phenomena by a high-resolution MM5 model showed that even smaller scale conditions are contained in synoptic scale patterns, represented in this case by the ECMWF model.

Keywords: Squall line; Supercell; MM5 meso-scale model

1. Introduction

Two significant types of severe convective phenomena can be observed in the Pannonian plain: squall lines and supercells. Sometimes squall lines themselves are able to generate supercells, sometimes individual supercells appear as prefrontal convective storms. Both types are difficult to predict and usually cause huge damages. The dynamics of these events as well as synoptic conditions necessary for their development have been described by Horvath and Geresdi (2003), but detailed numerical investigation was not made earlier, because the applied numerical models were hydrostatic. The PSU/NCAR meso-scale model MM5

* Corresponding author. Tel.: +385 1 4565 772; fax: +385 1 4565 757.

E-mail addresses: strelec@cirus.dhz.hr (N. Strelec Mahović), horvath.a@met.hu (A. Horvath), csirmaz.k@met.hu (K. Csirmaz).

[1] Tel./fax: +36 84 310 466.

0169-8095/$ - see front matter © 2006 Elsevier B.V. All rights reserved.
doi:10.1016/j.atmosres.2005.09.011

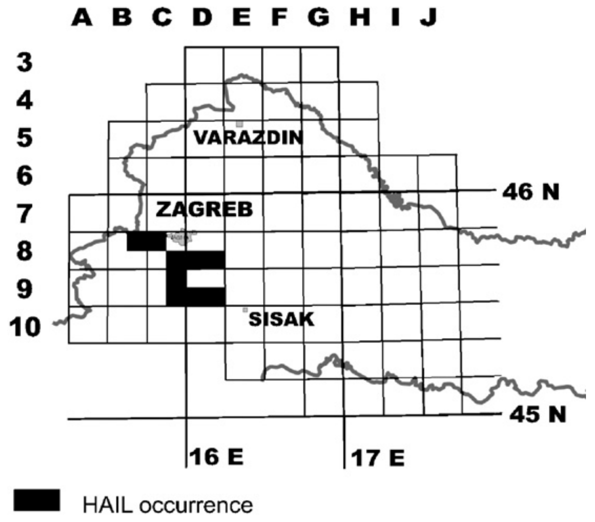

Fig. 1. Hail occurrence on 28 July 2003. The regions where hail was either observed or measured by hail-pads are marked.

(Grell et al., 1994) installed at the Hungarian Meteorological Service enabled the beginning of numerical experiments. The well developed cloud physics and planetary boundary layer schemes together with the non-hydrostatic dynamics of MM5 are more or less able to simulate the above mentioned severe convective events. Better results are obtained when the analysis nudging technique is applied for the first one or two hours of the model run. First guess data and boundary conditions are taken from ECMWF analysis and forecast, while synoptic data are introduced via nudging technique. Two numerical case studies are presented in this paper: a squall line affecting northwest Croatia and a supercell causing huge damages in the eastern part of Hungary.

2. The model

The applied numerical model, PSU/NCAR mesoscale model MM5 was installed on Silicon ORIGIN 2000 platform and run by 16 processors. The horizontal resolution of the model in both case studies was 3 km. ETA planetary boundary model (Janic, 1994), Reisner mixed-phase explicit moisture scheme (Reisner et al., 1998) and a rapid radiative transfer model for radiation scheme (Mlawer and Brown, 1997) were applied. The surface scheme was a five layer soil model (Dudhia, 1996). The first guess data, for the objective analysis, were taken from ECWMF analysis. The surface observations were introduced via analysis nudging in the first two hours of the model run. Lateral boundary conditions were taken from ECMWF forecast in such a way that every 3 h the original forecast is taken, meantime data were linearly interpolated.

3. Case studies

3.1. Squall line in northwest Croatia

In the evening hours on 28 July 2003, a squall line formed over north-western part of Croatia and western Hungary. Storm cells caused heavy rainfall, hail and strong winds. Several houses and dozens of cars were damaged by strong winds, hail destroyed numerous crop fields. Hail occurred in the regions west and south of Zagreb in the areas marked in Fig. 1. The observed average hailstone diameter was up to 22 mm with duration of hail from 2 to 15 min

Table 1
Hail observations

Year	Month	Day	Hour	Min	Duration (min)	Average radius (mm)	Quadrant	Damage
2003	7	28	20	5	10	7	B08	10%
2003	7	28	20	18	7	12	C08	5%
2003	7	28	20	20	5	10	C08	No
2003	7	28	22	50	5	12	C08	No
2003	7	28	22	43	2	16	D08	10%
2003	7	28	22	20	10	10	D08	No
2003	7	28	21	15	3	8	D09	5%
2003	7	28	21	25	15	18	C09	5%
2003	7	28	22	40	3	22	C09	10%
2003	7	28	21	43	4	12	D09	No
2003	7	28	23	20	2	12	C09	No
2003	7	28	23	30	2	12	D09	No
2003	7	28	22	20	5	10	B08	5%
2003	7	28	22	32	13	10	D08	10%

Duration of hailshowers, average hailstone diameter, location and damages are given. Quadrants listed in the table are depicted in Fig. 1.

Table 2
Hail-pad measurements

Year	Mon	Day	Hour	Min	Duration (min)	Max diameter (mm)	Number of hailstones	Average diameter (mm)	Total weight (g)	Quadrant
2003	7	28	20	20	3	12.6	1024	7.3	230.7	B08
2003	7	28	20	05	15	18.5	2848	9.5	1430.1	C08
2003	7	28	20	18	7	19.6	1280	10.1	832.8	C08
2003	7	28	22	43	17	23.4	1360	9.8	808.7	C08
2003	7	28	22	32	13	18.0	1008	9.3	507.1	D08

Maximum diameter and average diameter of hailstones as well as number of hailstones and total weight on each hail-pad are given.

(Table 1). According to the hail-pad measurements, given in Table 2, the maximum hailstone diameter was 23.4 mm. Accumulated rainfall during the event was from 20 to 60 mm in the regions south of Zagreb.

The conditions that preceded the formation of the squall line included a frontal system approaching across the Alps from the northwest, as seen in Fig. 2a. The region of interest was under the southwesterly upper-level flow on the leading side of a deep upper-level trough (Fig. 2b). However, in lower levels, up to 850 hPa, the flow was northeasterly, due to the influence of a low south of the Black Sea over Turkey and the high over northeast Europe.

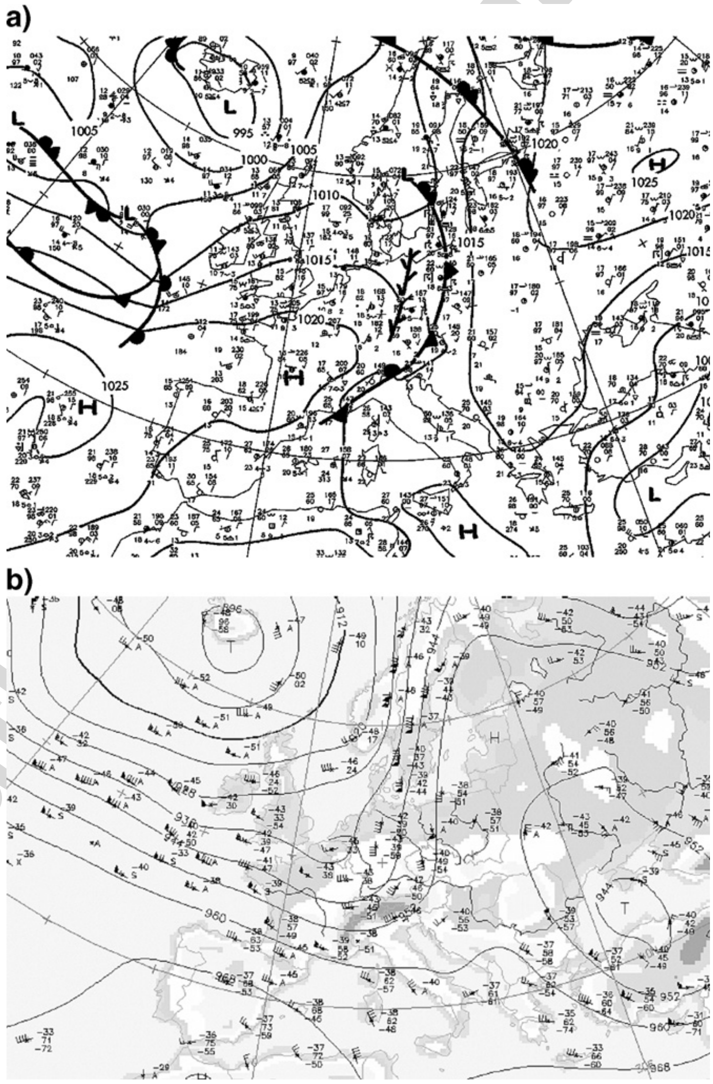

Fig. 2. DWD analysis on 28 July 2003 at 12:00 UTC: (a) surface weather map; (b) 300 hPa height and data from radiosonde measurements.

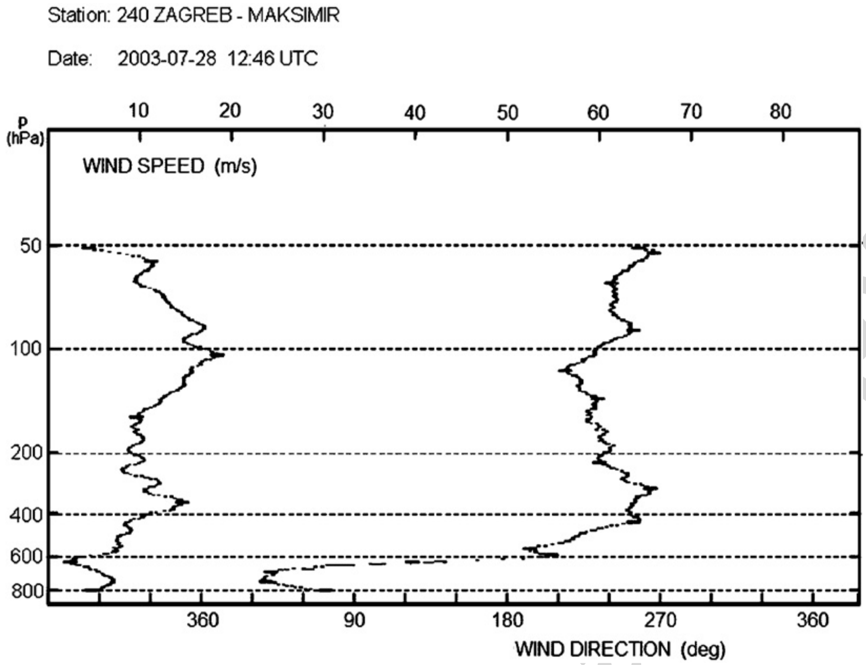

Fig. 3. Hodograph of Zagreb–Maksimir sounding on 28 July 2003, 12:00 UTC. Left line: wind speed (m/s), right line: wind direction (degrees).

According to the radiosonde measurement at 12 UTC over Zagreb, in the layer between 870 and 600 hPa there was a strong vertical speed and directional wind shear as seen in hodograph in Fig. 3. Also, temperature and humidity profile showed strongly unstable conditions. The veering of the winds with height in the first 4–5 km and the strongly unstable conditions were obviously favourable for convective development.

Development of the squall line started as prefrontal development in the late afternoon. Radar images in Fig. 4 show the formation starting from a single cell and developing into a well recognisable line of cells. A single cell developed at Croatian–Slovenian border with radar reflectivity higher than 50 dBZ at 18:15 UTC (Fig. 4a). An hour later a line of 4–5 cells could be observed over NW Croatia (Fig. 4b). From the appearance of the cells in radar imagery it seems that the energy of the first cell is transferred to the cells developing to the left of it. In other words the first cell generates circulation favourable for the development of the new cells to the left of the original one. By 21:00 UTC frontal cloud band already reached the squall line (Fig. 4c). After that the cells over Hungary decreased, whereas new developments were still going on over Croatia (Fig. 4d).

Looking at the results of the MM5 model simulation, some typical features of squall lines can be seen. In 850 hPa wind field at 21:00 UTC (Fig. 5a) the main cell shows a well developed vortex i.e. the circulation system typical for a supercell, whereas the other cells do not have the rotation. One hour later two other vortices developed on the left wing of the squall line (Fig. 5b). The model successfully simulated the effect observed in radar imagery: the new vortex develops stronger rotation whereas the original one gets weaker. At 23:00 UTC (Fig. 5c) the middle cell showed stronger rotation then the right one. At this point the development and strengthening of the individual cells is much more significant than the movement of the whole squall line.

Temperature field at 500 hPa also shows characteristic features. Very intensive updraft and extremely strong latent heat release generate strong warm cores at 500 hPa level (Fig. 6). Every warm core belongs to one cell and the horizontal temperature gradient of a given core depends on the development phase and the strength of the cell. The strongest core belongs to the oldest cell on the right wing of the squall line. The difference in temperature between the cell and the surrounding is 4 to 5 °C. The explanation of the warm cores at 500 hPa level can be found by looking at the vertical thermal structure of the squall line. In the cross-section in Fig. 7 it is indicated that between 900 and 400 hPa equivalent potential temperature (θ_e) is nearly constant, in this case about 60 °C, meaning that the entrainment of the outside air into the thunderstorm is very small, so the air parcels are rising wet-adiabatically.

This nearly constant value of θ_e allows including heavy thunderstorms into numerical models via initial conditions. In places where radar reflectivity shows heavy thunderstorms, θ_e can be taken as vertically constant value in the middle troposphere and the temperature profile can be calculated back to all pressure levels considering the relative humidity to be constant value (Horvath and Csirmaz, 2004).

Although the model simulated convective development quite well, it seems that it needs much more time to develop convective cells and the rotating structure, thus having shift in time compared to the real development. Besides that, the hourly accumulated precipitation forecast by the model is by far overestimated compared to radar estimated precipitation. In Fig. 5b the model forecasted hourly precipitation at 22:00 was up to 80 mm. On the other hand, radar estimated hourly values (Fig. 8) were not larger than 25 mm. The rain gauge data confirm the radar information: on almost all locations in the region of interest, total accumulated precipitation for that event was from 20 to 40 mm and only one station recorded as much as 60 mm but within 24 h.

3.2. Supercell in east Hungary

On 09 June 2004 a prefrontal supercell caused heavy storm in the eastern part of Hungary. This storm was not correctly predicted by the forecasters. Possible reason could be that the synoptic situation did not look dangerously because cold fronts coming from north to Hungary rarely cause severe convective events. The other reason could be the fact that the developing storm was not recognised as a supercell. Supercells are

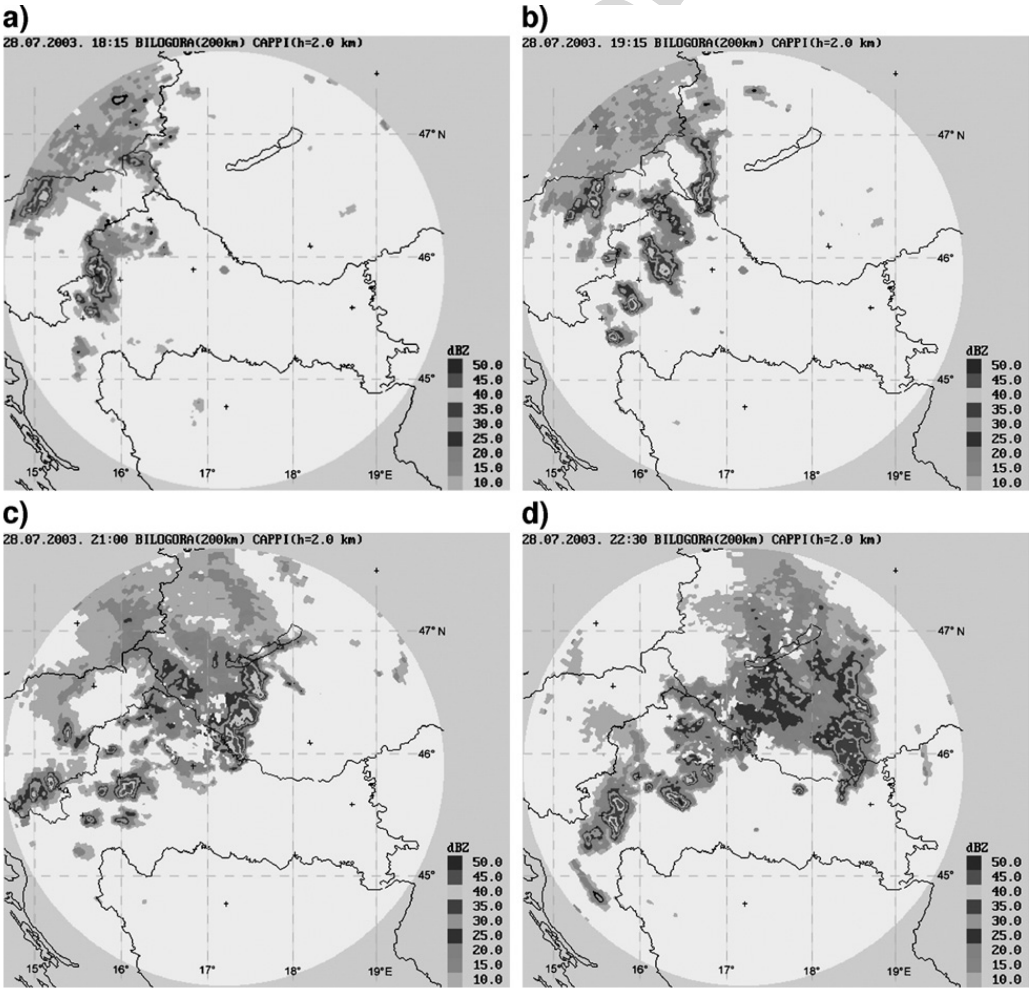

Fig. 4. Radar images for 28 July 2003: (a) at 18:15 UTC, (b) at 19:15 UTC, (c) at 21:00 UTC, (d) at 22:30 UTC; radar reflectivity (CAPPI at 2 km) in dBz is depicted.

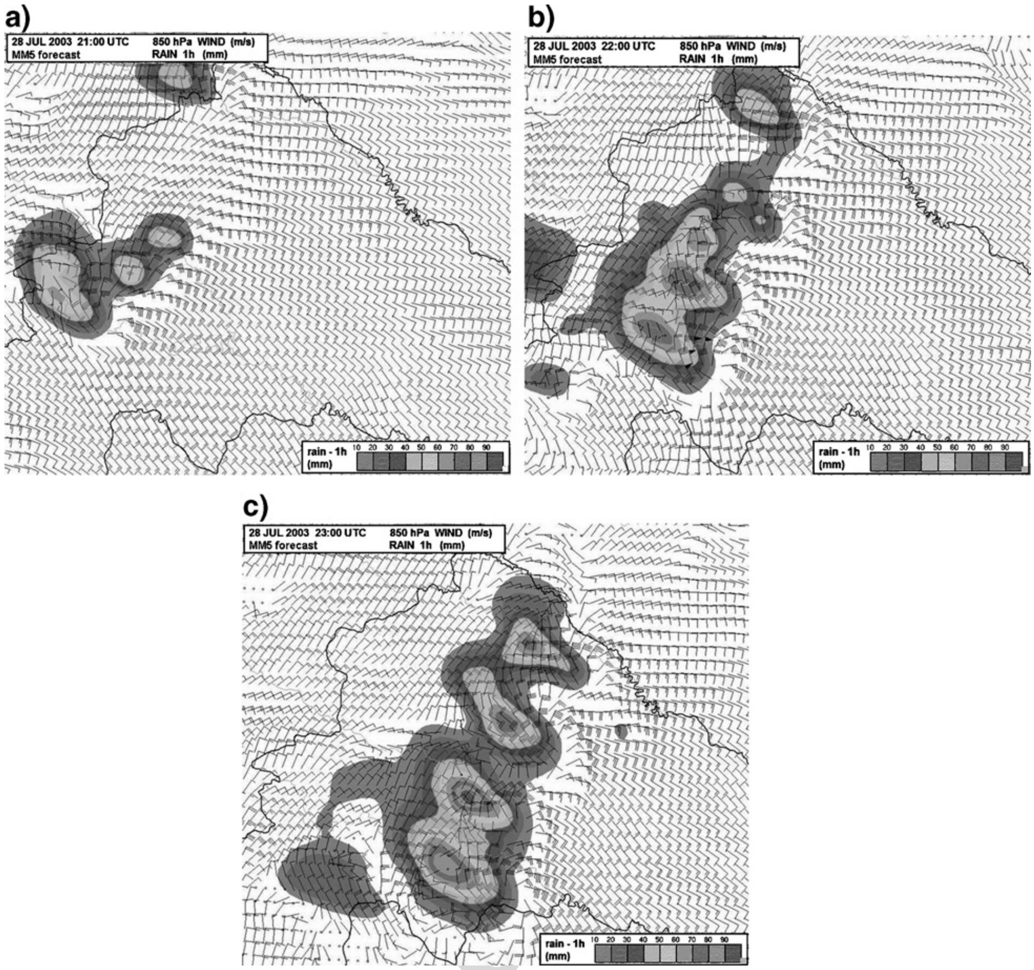

Fig. 5. MM5 model forecast of wind at 850 hPa and hourly accumulated precipitation for 28 July 2003 at (a) 21:00 UTC, (b) 22:00 UTC, (c) 23:00 UTC.

considered to be rather rare phenomena in this region, which is not necessarily true. In summer 2004 detailed investigation found at least six supercells and there were another four suspected cases. The case analysed here caused serious hail and wind damages. Tornado was not reported but from damage reports appearance of tornado is not excludable.

The synoptic situation from DWD analysis at 12:00 UTC showed a deep cyclone above East Europe and a sharp cold front approaching the Carpathian basin. Behind this front a northeast stream was building up (Fig. 9a). As a weather pattern it would have been a typical winter case when the East-Carpathians used to lead out low level cold air masses defending the Carpathian basin from polar air masses. The first waves of low level air masses really avoided the basin but in the upper levels the cold advection (Fig. 9b) could not have been lead out and it caused growing convective instability. The polar jet stream was also close to the investigated area and the wind shear caused favourable conditions for severe thunderstorms (Fig. 9c).

The first radar echoes indicating development of a thunderstorm appeared at 14:15 UTC. At 15:15 (Fig. 10a) radar reflectivity was greater than 60 dBz in the

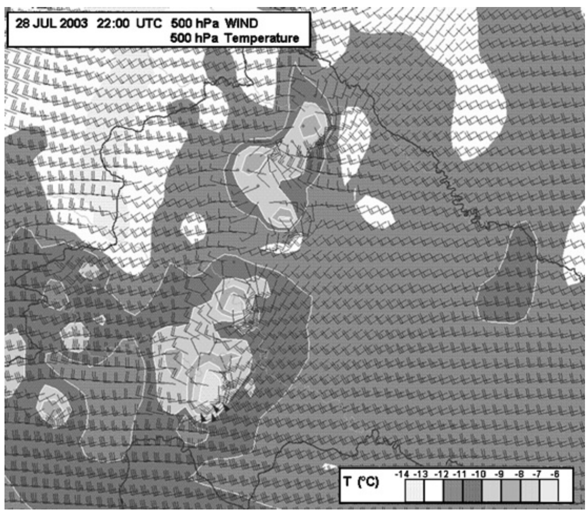

Fig. 6. MM5 model forecast of 500 hPa temperature and wind for 28 July 2003 at 22:00 UTC.

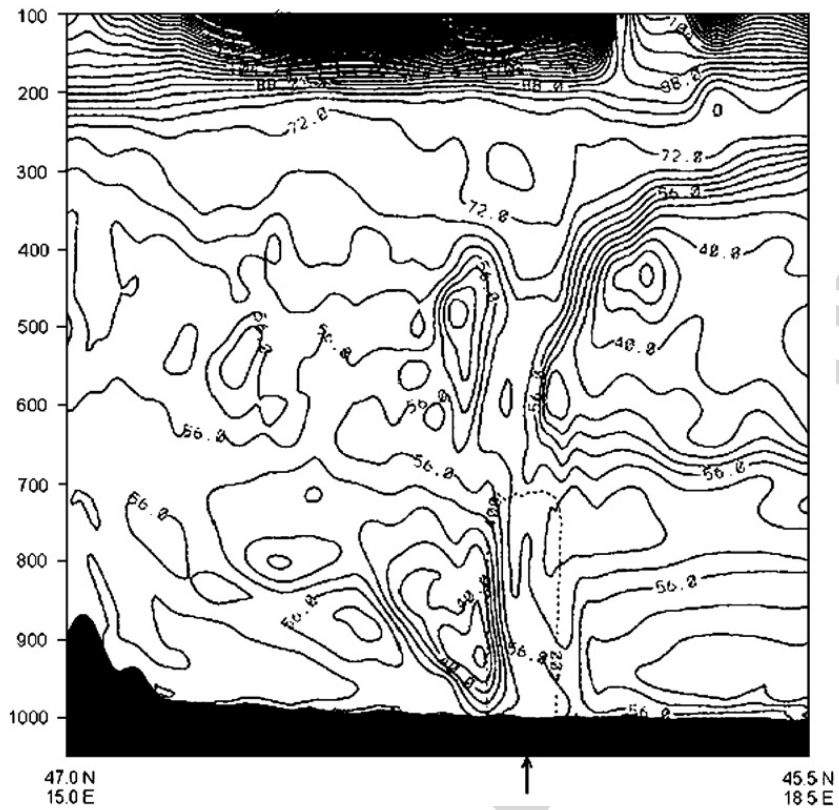

Fig. 7. Vertical cross-section along a line perpendicular to the squall line (geographic coordinates are indicated). Solid lines: equivalent potential temperature (°C) — every 4 °C; dashed lines: rain water; the region of nearly constant θ_e value is marked by an arrow.

centre of the storm. The cell already shows supercell appearance by its shape, with the weaker echo region to the right of the maximum signal. The storm moved to SSE direction and caused nut size hail and very strong wind. The speed of the cell was about 40 km/h and its maximum reflectivity changed from 56 to 65 dBz, as seen in Fig. 10.

Meanwhile the cold front broke into the basin and it also caused stormy wind and heavy thunderstorms. In radar images it can also be seen that the distance between the front and the squall line decreased but it did not affect the intensity of the storm.

The numerical simulation starts at 12:00 UTC, 2 h before the break out of the storm. At the time the thunderstorm began, at 14:00 UTC, the model predicted convective precipitation on the same place where it was in reality (Fig. 11a.). But besides that cell, the model developed some other precipitation areas west of the storm, whereas in reality there was no precipitation on those places. The hourly accumulated precipitation at 16:00 UTC, shown in Fig. 11b, indicated intensive storm. By that time that was the only ruling thunderstorm in the model field, the other unreal ones disappeared. By 18:00 UTC the hourly accumulated precipitation of the storm reached its maximum and new cells belonging to the cold front appeared on the north (Fig. 11c).

Detailed analysis of the wind field shows that at the beginning time there was no significant vortex connected to the thunderstorm. The first sign of vortex appeared at 16:00 UTC, getting more intense and larger

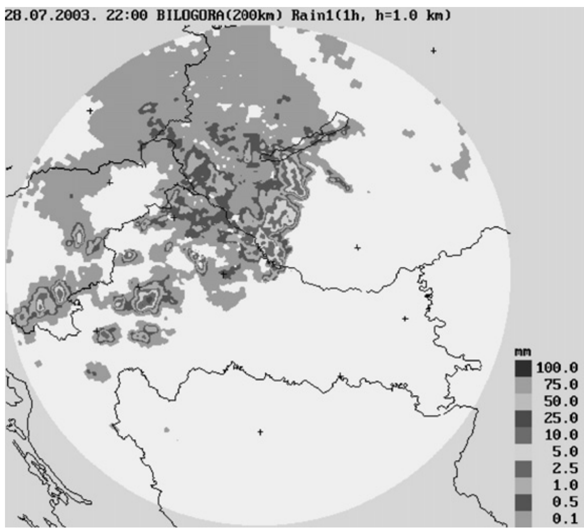

Fig. 8. Radar estimated hourly precipitation in the northwest Croatia on 28 July 2003 at 22:00 UTC.

by 18:00 UTC (Fig. 12). By that time a new vortex also appeared to the northwest of the main cell which shows some similarity to the previous case when vorticity “spread over” the convective system.

A cross-section of the developed supercell shows homogenous vertical θ_e values in the core of the storm. Additional to that a strong vertical circulation system can be clearly seen (Fig. 13).

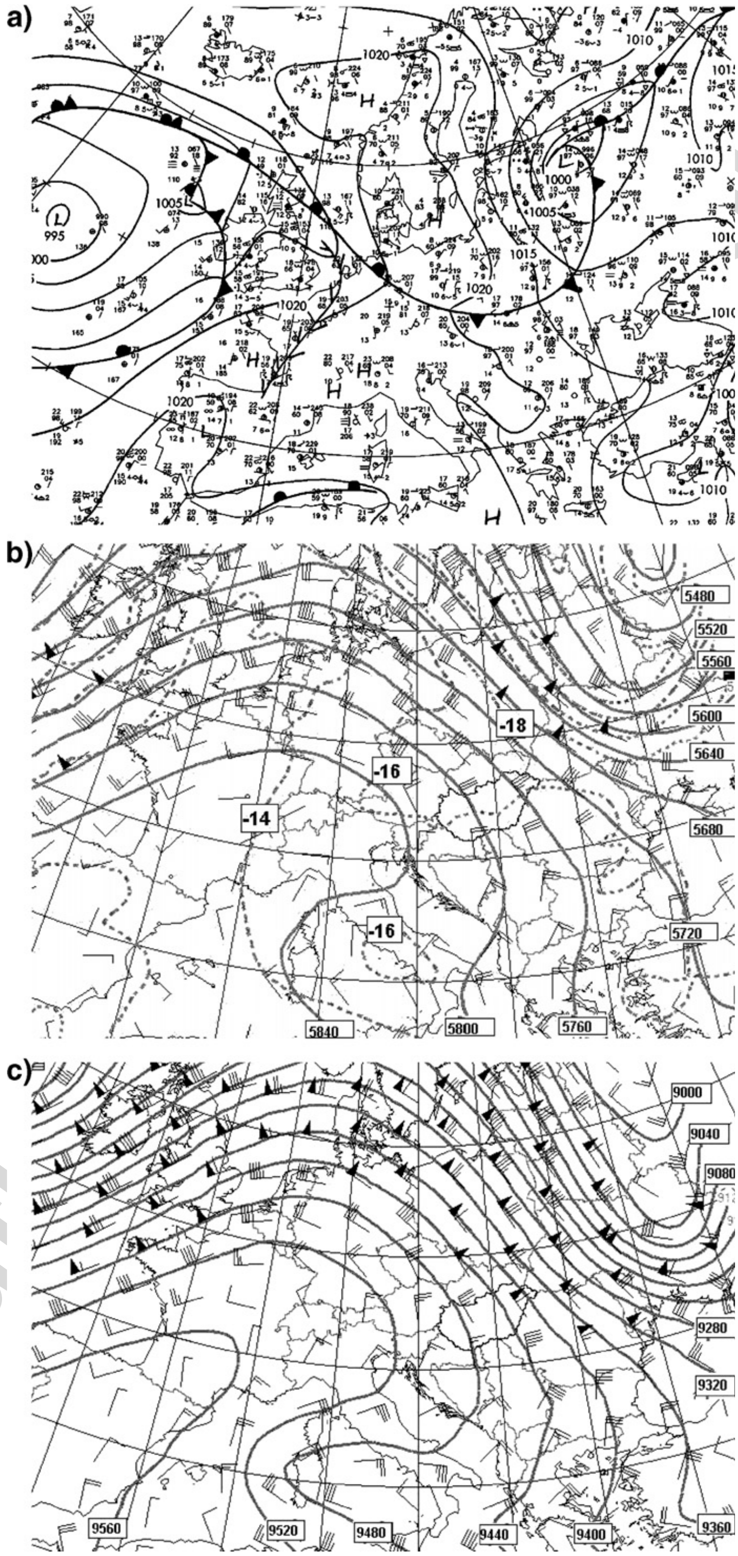

Fig. 9. Synoptic conditions on 09 June 2004 at 12:00 UTC: (a) DWD surface weather map; (b) 500 hPa height (solid lines), temperature (dashed lines) and wind from the ECMWF model; (c) 300 hPa height and wind from the ECMWF model.

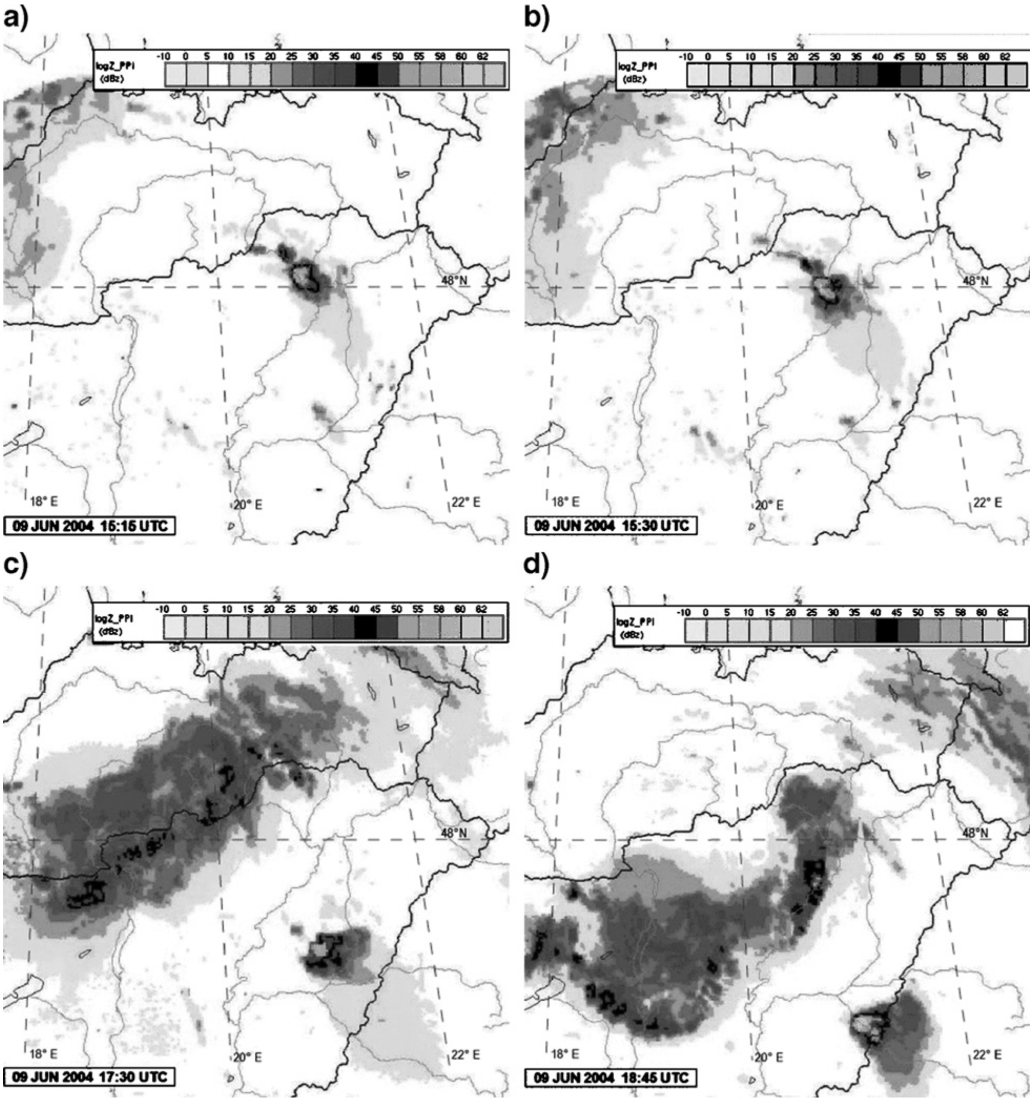

Fig. 10. Radar images of northeast Hungary for 09 June 2004 at (a) 15:15 UTC, (b) 15:30 UTC, (c) 17:30, (d) 19:45 UTC. Reflectivity (logZ_PPI) in dBz is depicted.

Comparing the model results with the real case, the model nearly exactly predicted the appearance, development and propagation of the severe thunderstorm. However, radar observations and other reports show that in the reality the supercell signatures appeared at least 1 h earlier than the significant vortex in the model. The model generated another rotating cell (similar to the first case study) but in reality radar observation indicated only one long living cell.

4. Summary and conclusions

In this paper numerical simulation of two types of severe convective phenomena is presented. In both cases the non-hydrostatic model MM5 was able to successfully simulate convective development. The first case, a squall line, was more characteristic and robust meso-alpha phenomenon. The model simulated the appearance of the system quite well. The vortices in the wind field and warm spots in temperature field successfully reproduce the characteristics of the real cells in the squall line. However, the model seems to need much more time to develop such a system than the nature. The second case, a single prefrontal supercell, was closer to the meso-gamma scale. The model predicted the appearance and the development of the cell, being again about an hour too late compared to reality.

In both cases the applied ECMWF data, which provided the main initial and full lateral conditions, had only 0.5° horizontal resolution. This resolution is enough only for meso-alpha scale non-hydrostatic modelling. However, the nested high-

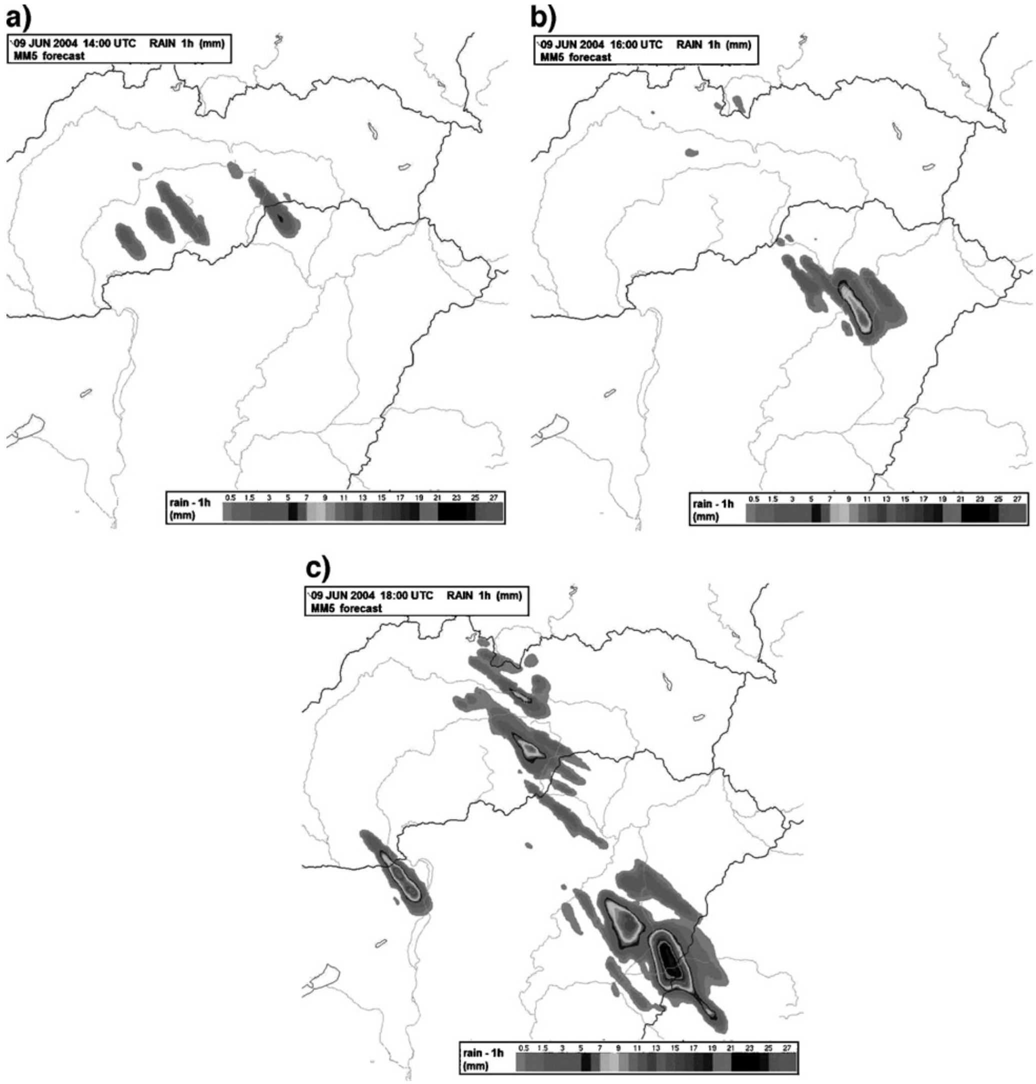

Fig. 11. Hourly accumulated precipitation forecast by MM5 for 09 June 2004 valid at (a) 14:00 UTC, (b) 16:00 UTC, (c) 18:00 UTC.

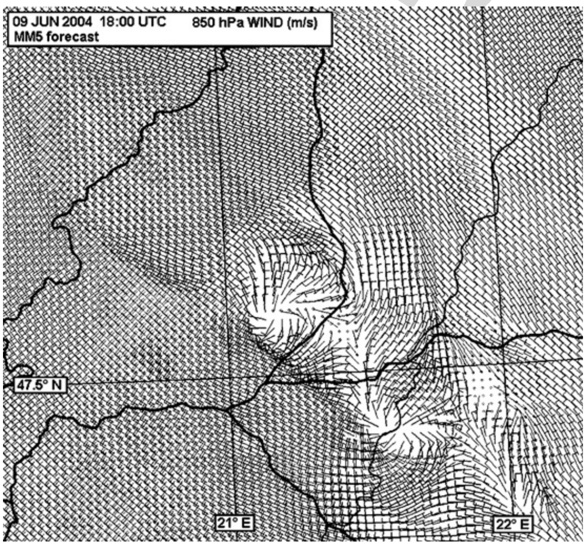

Fig. 12. MM5 model forecast of 850 hPa wind on 09 June 2004 at 18:00 UTC.

resolution model successfully reproduced the characteristics of convective phenomena without any additional smaller scale triggering. In other words the large scale model supported the appropriate condition for the meso-scale model to simulate meso-scale convective systems correctly. This successful simulation also indicates, that conditions for meso-scale development can be predicted by a large-scale model.

Acknowledgements

This work was supported by the Hungarian Scientific Research Fund under grant T043010 and by the Croatian Ministry of Science, Education and Sport in the framework of the national project "Storms and Natural Disasters in Croatia" (project No: 0004001).

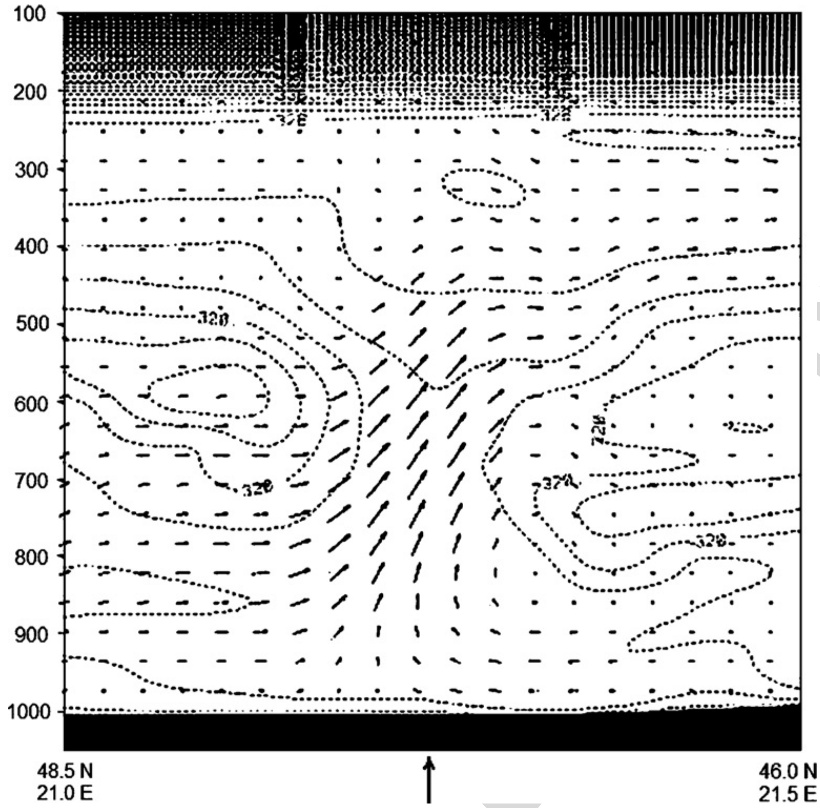

Fig. 13. Vertical cross-section through the cell (geographic coordinates are indicated). Dashed lines: equivalent potential temperature (K) — every 2 K (the region of nearly constant θ_e value is marked by an arrow); arrows: circulation vectors in cross-section plane.

References

Dudhia, J., 1996. A multi-layer soil temperature model for MM5. The 6th PSU/NCAR MM5 Users' Workshop Boulder Colorado, pp. 49–50.

Grell, G.A., Dudhia, J., Stauffer, D.R., 1994. A Description of Fifth-Generation Penn State/NCAR Meso-Scale Model (MM5). NCAR Technical Note, NCAR/TN-397+IA.

Horvath, A., Csirmaz, K., 2004. Assimilation of radar reflectivity data for triggering of convective phenomena. Proceeding of ERAD 2004, pp. 499–501.

Horvath, A., Geresdi, I., 2003. Severe storms and nowcasting in the Carpathian basin. Atmos. Res. 67-68, 319–332.

Janic, I., 1994. The step-mountain eta coordinate model. Mon. Weather Rev. 118, 1429–1443.

Mlawer, E.J., Brown, P.D., 1997. Radiative transfer for inhomogeneous atmosphere. J. Geophys. Res. 102, 16663–16682.

Reisner, J., Rasmussen, R.J., Bruintjes, R.T., 1998. Explicit forecasting of supercooled liquid water in winter storms using the MM5 meso scale model. Q. J. R. Meteorol. Soc. 124B, 1071–1107.